An Investigation on the Experimental Approach of Magnetic Properties and Magnetostriction

Research question: To what extent does an external magnetic field affect the magnetization of a material?

Physics

Word Count: 3688

I. Introduction

Magnetostriction is a critical property in many magnetic materials, playing an important role in various applications, from sensors and actuators to energy harvesting devices. While we study the concepts and significance of magnetism in ideal scenarios, it is also important to consider the magnetic properties subject to specific materials and to experimentally verify the theoretical phenomena to better understand the significance of magnetic properties. Thus, to provide a comprehensive view and deeper understanding of magnetostriction, this report aims to answer the research question, “To what extent does an external magnetic field affect the magnetization of a material?” through an experimental approach.

The magnetic hysteresis curve is one of the most important properties that differentiate a ferromagnetic material from a diamagnetic or paramagnetic material. For a diamagnetic and paramagnetic material, when present in an external magnetic field, the material's magnetization (magnetic moment per unit volume) is proportional to the external magnetic field. In the diamagnetic case, magnetization is the opposite sign of the external magnetic field. In the paramagnetic case, magnetization is of the same sign. For ferromagnetic materials, the relationship between the applied (external) magnetic field H and the magnetization field M is more complex. As H increases, initially, M increases linearly, much like a paramagnetic material. But for higher values of H, the magnetization of the material saturates, and M will asymptotically approach a maximum/minimum. The relationship between H and M can be used to characterize materials. Determining a material’s H-M relationship is of practical importance. In many devices like motors and transformers, the magnetic material should operate in the linear region of the H-M to achieve high efficiency. Engineers must select the material with a suitable H-M characteristic to meet design requirements.

Magnetostriction is responsible for some undesired properties in electromagnetic systems. A prime example is the humming noise often heard near power transformers. When a magnetic field penetrates the ferromagnetic core of a transformer, the core changes in dimension at a frequency twice that of the changing magnetic field. The core couples with surrounding structures and air to produce an audible sound. Depending on the system, the sound could be of a high frequency. For example, in switchmode power supplies, this effect is not only disturbing for users but is also a source of power loss. The challenge of measuring magnetostriction is in capturing the minute changes in material dimension. Typically, magnetostriction only alters the material dimension by a few parts per million (ppm). This necessitates sensitive instrumentation capable of resolving submicron changes in material dimension that can reject environmental electromagnetic interference.

In the first part of this report, an experimental setup is described that is capable of generating a controlled magnetic field in a small region of space by a solenoid and can simultaneously measure the combined magnetic field generated by the solenoid and the induced magnetic field caused by the magnetization of the material under test. The combined magnetic field B is measured by a Hall effect sensor. A detailed analysis of the B-H curves, ferromagnetic, and paramagnetic materials is presented. The response of different materials to an external magnetic field and at what field strength their magnetization saturates is explored. In the second part of this article, an attempt is made to quantify the magnitude of magnetostriction by performing a sensitive measurement of the strain (ratio of the change in length and the original length) of the material under different magnetic field strengths using a strain gauge apparatus.

Through these sections, this report investigates the magnetic properties of various materials. The focus is on two properties, specifically, the non-linear magnetization properties of ferromagnetic materials (magnetic hysteresis) and magnetostriction (when a magnetic material changes its dimensions when an external magnetic field is applied.)

II. Theoretical Background of B-H Curve

A. B-H curve of Ferromagnetic Materials (Ekreem, 2017, Storr, 2023 and Dhanyaprabha, 2023)

Ferromagnetic materials can usually be easily magnetized due to their high permeability. Thus, the magnetic flux density (B) is expected to increase when the magnetic field strength (H) increases.

We can quantify the axial magnetic flux density using Faraday's Law:

$$V(t) = NA\frac{dB}{dt} \quad [1]$$

where N is the number of turns for the coil and A is the cross-sectional area of the specimen in m^2.

To better incorporate the geometry of the specimen, we need to calculate dB and H inside the specimen. H can be calculated with the sum of the applied field (H_0) and the field generated by the magnetic pole distribution (ρ_m),

$$H_{in} = H_0 + \rho_m = \frac{B_0}{\mu_0} - div(\vec{M}) \quad [2]$$

where μ_0 is the vacuum permeability, H is the magnetic field strength, M is magnetization.

The magnetic flux density can be further calculated by

$$B = \mu H = \mu_0(H + M) \quad [3]$$

$$\frac{\mu}{\mu_0}H = (H + M) \quad [4]$$

through rearranging,

$$M = (\mu_R - 1)H \qquad [5]$$

where μ_R is the relative permeability.

Eq. [3] suggests that the magnetic flux density (B) is directly proportional to the magnetic field strength (H), where the proportionality constant is the absolute permeability of the material (μ).

Eq. [5] suggests the magnetization of the material (M) is directly proportional to the magnetic field strength (H).

Graphically, starting from the origin where both B and H are zero, a magnetization curve will be observed when B increases as a response to the increase of H. This is the magnetization stage, where the magnetic domains begin to align (shown in Fig. 1), causing an expansion in the material's dimensions.

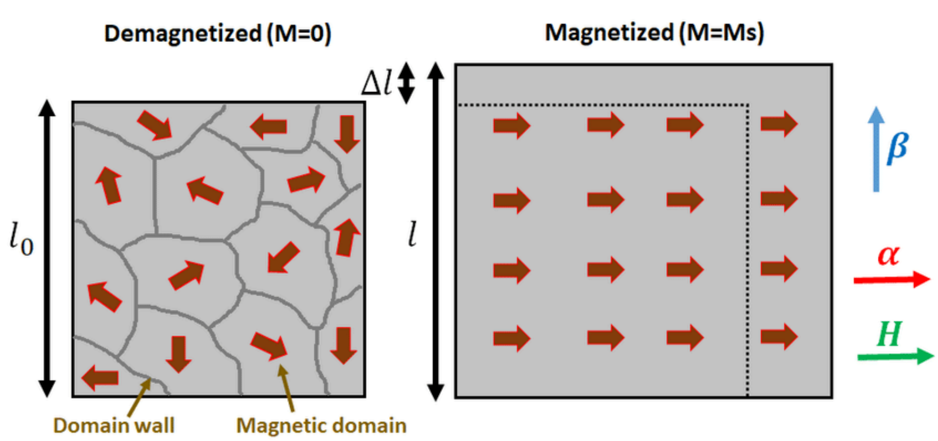

Fig. 1 Magnetic Domain Alignment

In summary, for ferromagnetic materials, the magnetic flux density is influenced by both the external magnetic field applied and the material's magnetization to that field. When almost all of its magnetic domains are aligned, and the magnetic material can't be further magnetized, the B-H curve will enter a plateau stage, known as the saturation state. If H is further increased in the negative direction, B will decrease and eventually reach a negative saturation. When H is then increased in the positive direction, B will follow a path different from the initial curve, forming a loop known as the hysteresis loop.

The hysteresis loop is significant in the study of magnetic materials since it acts as a signature of a material. For example, the area within the hysteresis loop can be used to calculate the energy lost as heat during the cycle of magnetization, which is subject to different materials.

B. B-H curve of Diamagnetic Materials (Bian, 2016)

Due to the negative magnetic susceptibility and the tendency to oppose an applied magnetic field of diamagnetic materials, they usually have a negative slope of the B-H curve. In addition, depending on the material's permeability, the permeability slope is often less than the vacuum permeability.

C. B-H curve of Paramagnetic Materials (Plouffe, 2014)

Paramagnetic materials are characterized by their positive magnetic susceptibility and their magnetic domain's tendency to align weakly with the applied magnetic field.

For paramagnetic specimens, its magnetization can be expressed as

$$M = \chi_m H \qquad [6]$$

where χ_m is the magnetic susceptibility of the material.

Substituting eq. [6] into eq. [3], we get

$$B = \mu_0(1 + \chi_m)H = \mu H \quad [7]$$

where $\mu = \mu_0(1 + \chi_m)$.

Based on eq. [7], the slope of the B-H curve of paramagnetic specimens is equal to its permeability.

To account for the impacts of temperature and saturation behaviour at high fields, Langevin's Theory can be used to further characterize the magnetization of paramagnetic materials,

$$M = \frac{n\mu^2 H}{kT} coth\left(\frac{\mu H}{kT}\right) - \frac{n\mu^2 H}{kT} \quad [8]$$

Where n is the number of magnetic moments per unit volume, μ is the magnetic moment of each atom or ion, k is Boltzmann's constant, T is the absolute temperature in Kelvin, and coth is the hyperbolic cotangent function.

Because Langevin's Theory uses the hyperbolic cotangent function, it can be used to determine the non-linear response of individual magnetic moments to the external field, which is very useful in the understanding of magnetic behaviour at varying temperatures and high magnetic fields.

III. Theoretical Background of Magnetostriction

Ferromagnetic materials consist of magnetic domains. Each domain is a region where the magnetic moments of atoms are aligned in the same direction. In the absence of an external magnetic field, these domains are randomly oriented, resulting in no net magnetization. When a magnetic field is applied, these domains tend to align with the field, changing the material's dimensions.

Magnetostriction can be expressed in terms of Joule's magnetostriction coefficient (λ),

$$\lambda = \frac{\Delta L}{L} \quad [9]$$

A. Relation to Magnetic Field Strength

The change in length, ΔL, is proportional to the square of the magnetization, M, of the material:

$$\Delta L = \lambda L_0 M^2 \quad [10]$$

where M is given by $M = \chi H$.

Here, χ is the magnetic susceptibility of the material, L_0 is the initial length of the material, and H is the magnetic field strength.

Combining the eqs. [9] and [10], we get:

$$\Delta L = \lambda L_0 (\chi H)^2 \quad [11]$$

B. Expansions (Pacewicz, 2023)

Since magnetostriction does not occur uniformly through the entire specimen, both longitudinal expansion ($\lambda_{\parallel}$) and transverse expansion ($\lambda_{\perp}$) need to be considered, thus the internal magnetic field induced driving torque (τ_D) is a combination of both dissipating torque (τ_E) and restoring torque(τ_K), thus

$$\tau_D = \tau_E + \tau_K \quad [12]$$

given $\tau_E = -\ \beta(\frac{d\theta_L}{dt})$ and $\tau_K = (\frac{K}{M})\frac{sin\,(2(\delta - \theta_L)}{sin\theta_L}$, where β is the coefficient that represents the strength or effectiveness of the eddy current torque, $\frac{d\theta_L}{dt}$ is the rate of change of the angular position (θ_L) with respect to time, K is the magnetic anisotropy constant, and δ is the preferred direction of magnetization for the material.

Substitute,

$$\tau_D =- \beta(\frac{d\theta_L}{dt}) + (\frac{K}{M})\frac{sin(2(\delta-\theta_L)}{sin\theta_L} = H \qquad [13]$$

where H is the driving magnetic field.

Considering both the longitudinal direction and the transverse direction, the driving magnetic field can be expressed with respect to frequency dependence in both directions

$$H = \beta(\frac{d\theta_T}{dt}) - (\frac{K}{M})\frac{sin(2(\delta-\theta_T)}{cos\theta_T} - \beta(\frac{d\theta_T}{dt}) \qquad [14]$$

where $\theta_L + \theta_T = \frac{\pi}{2}$.

With the frequency doubling, the magnetostrictive strain signal can be expressed using the even cosine function,

$$\lambda(t) = \frac{3}{2}\lambda_0(cos^2\theta(t) - \frac{1}{3}) \qquad [15]$$

where λ_0 is a constant representing the maximum possible magnetostrictive strain in the material.

With $cos^2\theta(t)$ doubling the frequency of the strain response compared to the applied magnetic field, eq. [15] successfully scales and normalizes the strain response, which characterizes the magnetostrictive strain in a material as a function of time, taking into account the frequency doubling effect.

IV. Measurement of B-H Curve

A. Experimental Apparatus

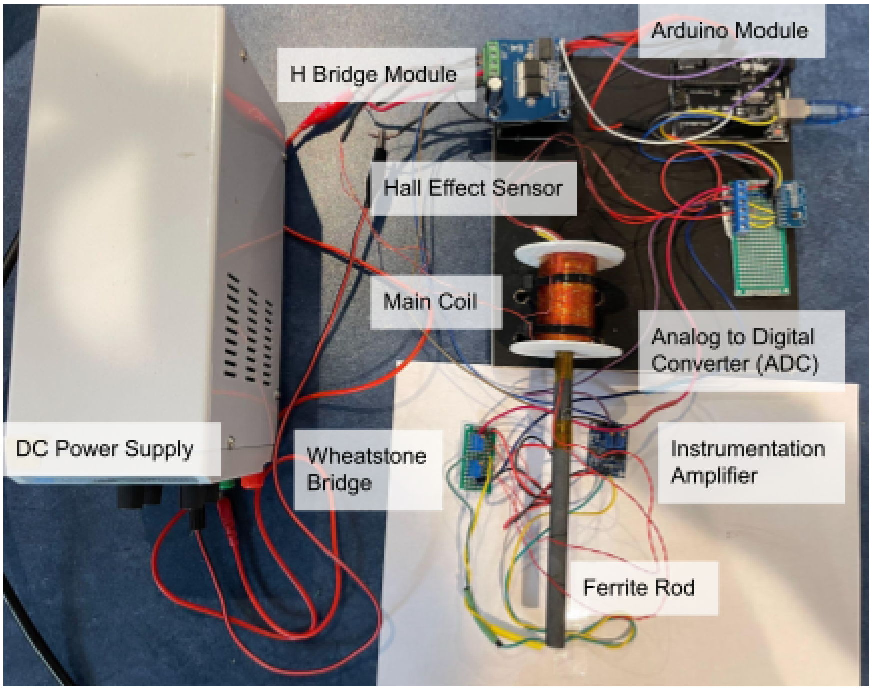

Fig. 2 Main Experimental Setup

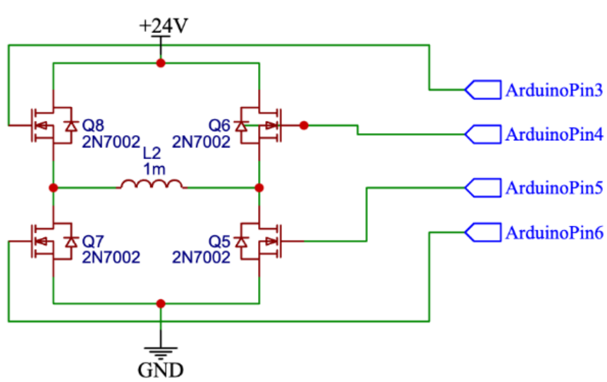

Fig. 3 Schematic of B-H Curve H-Bridge Setup

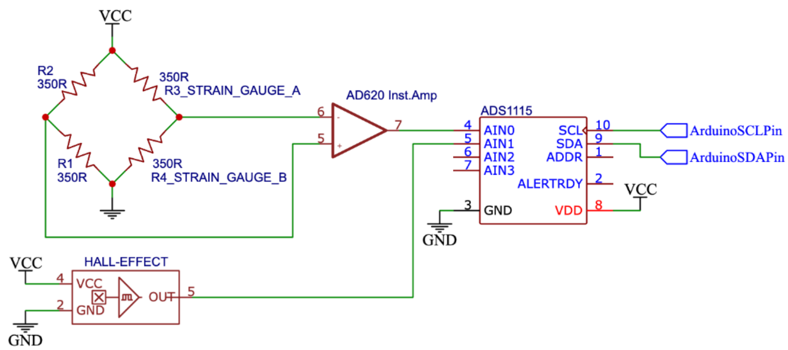

Fig. 4 Schematic of Magnetostriction Strain Gauge Setup

1. Coil

The main coil shown in Fig. 2 is responsible for generating the magnetic field. This solenoid consists of 1100 turns of 24 AWG (American wire gauge) enamelled copper wire in 13 layers. The enamel (insulating coating covering the wire) provides electrical insulation for temperatures up to 150°C and the layers of wires are secured with Kapton tape - a type of tape commonly used to insulate high-temperature electronics. The solenoid has a length of 10 cm with a 1 cm diameter hollow core, in which the core houses the magnetic material under test. For this solenoid specifically, with a current of 3 A, it can generate a magnetic field of roughly 40 mT with an air core.

2. H-bridge

Fig. 3 is a detailed schematic of the h-bridge built for this report's experiments. An H-bridge circuit is used to control the current through the solenoid. It consists of four transistors known as MOSFETs (metal oxide semiconductor field effect transistors). These transistors are electronic switches controlled by voltage, meaning that if two diagonal transistors are switched on, the current will flow through the coil (denoted in the schematic by an inductor) in one direction. If the other two diagonal transistors are switched on, the current will flow in the opposite direction. This is helpful to apply a positive and negative magnetic field to the material under test without reconnecting any electronics. One additional feature of the H-bridge is its ability to control the magnitude of current flow, which allows a fixed voltage to go across. By modulating the current flow using pulse-width modulation (only switching on the MOSFETs in pulses for varying amounts of time), the on-time of the H-bridge and, thus, the time-averaged current through the solenoid can be controlled. Since the solenoid is an inductor, it will reject rapid changes in current. If the modulation frequency is set to be sufficiently high, the current through the solenoid is nearly ripple-free.

3. Linear Ratiometer Hall Effect Sensor

A linear ratiometric Hall effect sensor is mounted on the end of the solenoid to measure the combined magnetic field generated by the solenoid and by the magnetization of the material. The sensor uses the Hall effect, which states that when a magnetic field penetrates a material with a longitudinal electric current, there will be an electric field in the transverse direction proportional to the magnetic field strength. The sensor utilizes this effect to produce a voltage output proportional to the magnetic field, and the voltage output can then be measured and digitized by an analog-to-digital converter (ADC).

4. Materials to be Measured

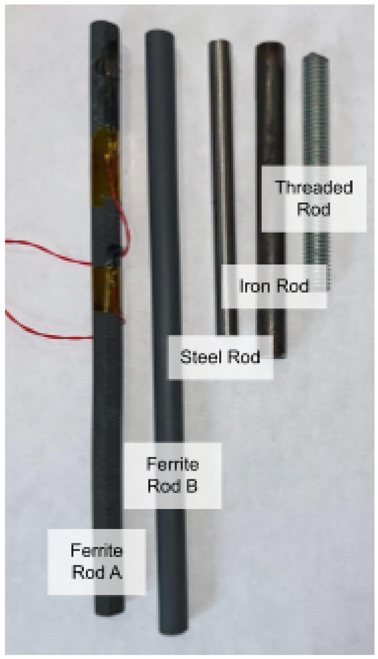

Fig. 5 Materials Measured

Various materials are chosen, and the materials are expected to demonstrate different magnetic behaviours through their B-H curve.

B. Results

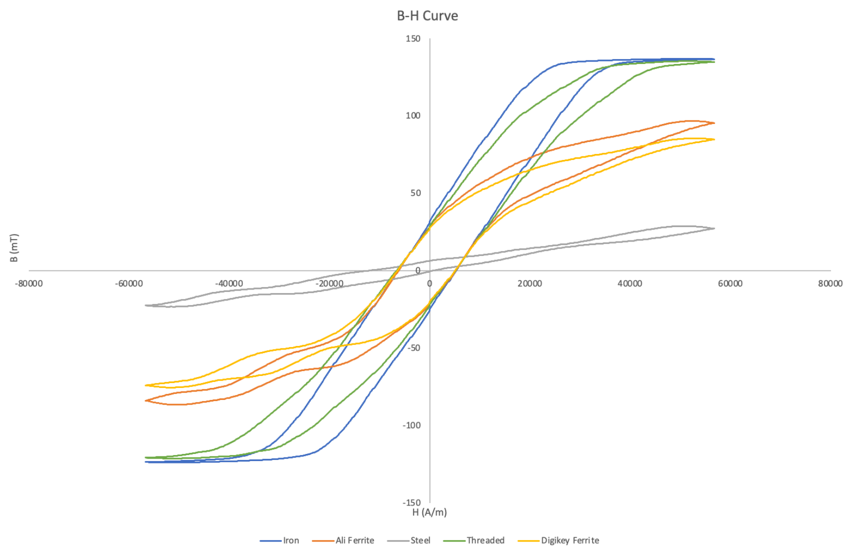

Fig. 6 Hysteresis Loop of Magnetic Materials

As shown in Fig. 6, iron rod and threaded rod have the highest saturation point, followed by the two types of ferrite rod and steel rod having the lowest maximum point and no saturation state. This confirms the theory that only ferromagnetic materials demonstrate hysteresis loop and magnetization saturation, as discussed in Sec. II.

The higher saturation magnetization of threaded rod and iron rod also shows that they can achieve a higher maximum magnetic flux density before being fully magnetized compared to the material of ferrite rod.

The difference in H required for saturation means the material requires a different amount of magnetic field to cause full expansions; based on the materials tested in this report, iron needs the least amount of magnetic field, followed by the threaded rod, followed by the ferrite rods.

The difference in the slope of the B-H curve also suggests the difference in magnetic permeability between the measured materials. In this experiment, iron and threaded rods have the steepest slopes, suggesting that these materials can easily be magnetized by an external magnetic field, which makes them suitable materials for transformers and inductors. On the other hand, ferrite has flatter slopes, meaning that ferrite is less responsive to external magnetic fields.

C. Discussion/Limitations

Overall, the B-H curve measurement provided insights into the magnetic properties of the measured materials, which could be beneficial when determining the desired application of materials. However, there are limitations in this experiment that could affect the accuracy of the results. For example, the coil has a relatively weaker magnetic field due to the difficulty of winding coils at home, which makes it unable to show the saturation of some materials. Additionally, unlike AC experiments, the quasi-DC experiment used in this report has a limited sweep rate, which may also impact the accuracy of the result since it introduces time dependencies and temperature parameters that can not be precisely controlled.

V. Quantification of Magnetostriction in Ferrite Rod

A. Experimental Apparatus

1. Strain Gauge

A strain gauge is a type of variable resistor where its resistance varies with how much the device is elongated (strain). If a strain gauge is attached to a material and the material dimension changes, the change in dimension can be quantified by measuring the resistance of the strain gauge attached to it.

2. Wheatstone Bridge circuit

   Detailed schematic shown in Fig. 4. A Wheatstone bridge consists of four resistors. A voltage can be applied across the upper and lower terminals of the Wheatstone bridge and measure the voltage across the left and right terminals. For voltage across the bridge to be zero, the product of the resistor value of the two diagonal resistors must be equal. If some of the resistors are replaced with variable resistors, the resistance of the potentiometer can be deduced by measuring the voltage across the left and right terminals.

3. Instrumentation Amplifier

   An instrumentation amplifier is a device that consists of several operational amplifiers, and it mainly amplifies the voltage difference between its input terminals at the output. Compared to other amplifier topologies, an instrumentation amplifier has the advantages of very high input impedance (almost no current can flow into the amplifier) and excellent common mode rejection (only amplifies voltage difference and not voltage change common to both inputs). These characteristics make the instrumentation amplifier an excellent choice for amplifying weak differential mode signals (such as the signal from Wheatstone bridge) in an environment with electromagnetic interference (most of which are common mode noise).

4. Preliminary experiment

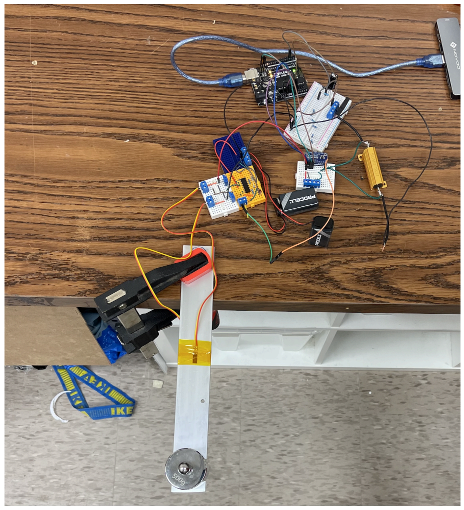

Fig. 7 Strain Gauge Calibration

In Fig. 7, a strain gauge system is used to measure the oscillation amplitude. An Arduino is connected to two paired strain gauges that are taped onto a metal piece, and a calibration weight is placed on one end of the metal piece to collect the signals of bending magnitude. The strain gauge allows for accurate measurement of any displacements with reference to the calibrated equilibrium, allowing for small measurements from the magnetostriction displacements.

B. Results

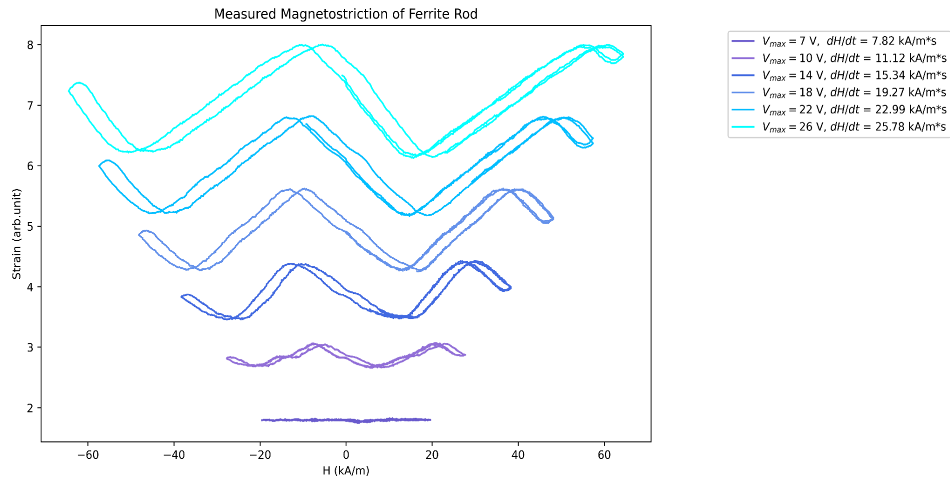

Fig. 8 Magnetostriction of Ferrite Rod

As shown in Fig. 8, the strain of material does depend on the magnetic field applied (as discussed in Sec. III), as we can see the butterfly shape of strain against H. This is highly non-trivial because the magnetic domain alignment is usually assumed to maintain its maximum extension after being magnetized. However, this phenomenon can be explained by the reversal property of the magnetic domain and the material's tendency in energy minimization, meaning that when the field is reduced, the material seeks to minimize its energy again, leading to a shrink in dimensions. In addition, as the current is increased, the rate at which the magnetic field is applied changes correspondingly, which can turn on magnetostriction and rule out environmental interference.

C. Discussion/Limitations

In this experiment, arbitrary units have to be used because the gain of the gain resistor is highly sensitive, which could vary by manufacturer and environmental conditions such as temperatures. This leads to the difficulty in calibrating the strain gauge and amplifier gain. However, this can be resolved by using an oscilloscope, which can better quantify the gain. Furthermore, the magnetostriction of other materials tested in Sec. IV was not quantified because those materials lack a flat face to epoxy the strain gauge on; this can be resolved through machinery to machine a flat edge onto the other hard materials like steel.

VI. Resonance Frequency of Magnetic Materials (Yalcin, 2013 and Xu, 2019)

Magnetostrictive resonance is another significant component under the concept of magnetostriction. Magnetostriction will only reach a constant frequency when the AC frequency is on the same order of magnitude as the magnetic materials' resonance frequency. When they are at relatively the same frequency, a resonance is reached from the core of the magnetic materials, thus resulting in constructive waves and leading to a higher amplitude of oscillation within the material.

Characterization of the magnetic moment in a magnetic material contributes to the resonance frequency, which can be expressed as

$$\frac{1}{\gamma}\frac{d\vec{M}}{dt} = \vec{M} \times \vec{H}_{eff} \qquad [16]$$

where γ is the gyromagnetic ratio and $\vec{H}_{eff}$ is the effective magnetic field, the cross product of magnetization and effective magnetic field indicates that the magnetization precesses around the direction of the effective magnetic field.

The right side of the equation above can be expressed in three different forms,

i) The Bloch-Bloembergen form: $-\frac{\vec{M}_{\theta,\varphi}}{T_2} - \frac{M_z \vec{-} M_0}{T_1}$

ii) The Landau-Lifshitz form: $\frac{-\lambda}{\left|\vec{M}\right|^2}\vec{M} \times \vec{M} \times \vec{H}$

iii) The Gilbert form: $\frac{\alpha}{\left|\vec{M}\right|}\vec{M} \times \frac{d\vec{M}}{dt}$

where α is the dimensionless damping parameter, T_2 is the transverse relaxation time, T_1 is the longitudinal relaxation time, $\vec{M}_{\theta,\varphi}$ is transverse magnetization components, M_z is the longitudinal magnetization component, and M_0 is the equilibrium magnetization.

The fundamental difference between these three forms is that they are each applicable under certain conditions. When α in the Gilbert form is small, all three forms are essentially the same. However, that means the $\vec{M}$ excursion must also be small and conserved since it is not protected.

For ferromagnetic materials specifically, the internal anisotropy energy must be considered when calculating the resonance. From the Bloch-Bloembergen equation and eq. [16], we get

$$\frac{1}{\gamma}\frac{d\vec{M}}{dt} = \frac{\vec{M}}{\left|\vec{M}\right|} \times \vec{\nabla} E - \frac{\vec{M}_{\theta,\varphi}}{\gamma T_2} - \frac{M_z - \vec{M}_0}{\gamma T_1} \quad [17]$$

where the energy density is

$$\vec{\nabla} E = -\left(\frac{\partial E}{\partial \theta}\right)\hat{e}_{\phi} + \frac{1}{sin\theta}\left(\frac{\partial E}{\partial \theta}\right)\hat{e}_{\theta} \quad [18]$$

assume the deviation from the equilibrium is small and may be negligible, the magnetization can be approximated by

$$\vec{M} = M_s\hat{e}_r + m_\theta \hat{e}_\theta + m_\phi \hat{e}_\phi \quad [19]$$

which can be decomposed into transverse components,

$$m_\theta(z,\ t) = m_\theta^0 exp\ i(\omega t \pm kz) \quad [20]$$

$$m_{\phi}(z,\ t)\ = m_{\phi}^{0} exp\ i(\omega t\ \pm\ kz) \quad [21]$$

A. Resonance Frequency for Longitudinal Expansion (f_{rL})

Resonance frequency for longitudinal expansion can be derived from the wave equation for longitudinal waves in a rod:

$$\frac{\partial^2 u}{\partial x^2} = \frac{1}{v^2}\frac{\partial^2 u}{\partial t^2} \quad [22]$$

where u is the longitudinal displacement and v is the speed of the wave, given by $v\ = \sqrt{\frac{Y}{\rho}}$, with Y being Young's modulus and ρ the density.

For a rod of length L, the fundamental resonance frequency is

$$f_{rL} = \frac{v}{2L} \quad [23]$$

B. Resonance Frequency for Transverse Expansion (f_{rT})

Resonance frequency for transverse expansion can be derived from the wave equation for transverse waves in a rod:

$$\frac{\partial^2 w}{\partial x^2} = \frac{1}{c^2}\frac{\partial^2 w}{\partial t^2} \quad [24]$$

where w is the transverse displacement, c is the speed of the wave, given by $c\ = \sqrt{\frac{G}{\rho}}$ with G being the shear modulus.

For a rod of diameter D, the fundamental resonance frequency is

$$f_{rT} = \frac{c}{\pi D} \quad [25]$$

C. Summary

The application of a magnetic field can modify the mechanical properties of the material, such as its Young's modulus and shear modulus, which then affects the resonance frequencies f_{rL} and f_{rT}. When the magnetic domain changes due to the magnetic field applied, the stiffness of the material changes accordingly due to the rearrangement of magnetic domain alignment. As the magnetic field strength increases, a point is reached where most of the magnetic domains are aligned, and the material becomes magnetically saturated. Beyond this point, further increases in the magnetic field do not produce significant changes in magnetization or strain. Consequently, the resonance frequency tends to stabilize or even decrease beyond magnetic saturation.

VII. Conclusion

Experimentally characterizing magnetic materials and measuring magnetostriction has been successful, as the empirical data aligns with established theory. In this report, the magnetic properties of ferromagnetic, paramagnetic, and diamagnetic materials are examined. This includes their distinct characteristics on the B-H curve when subjected to an external magnetic field. Among the three types of magnetic materials, only ferromagnetic materials exhibit non-linear magnetic properties, displaying a complete hysteresis loop when a magnetic field is applied. In contrast, both paramagnetic and diamagnetic materials exhibit linear properties, indicating a linear B-H curve relationship. For paramagnetic materials, due to their permanent magnetization properties, they exhibit a slope equivalent to vacuum permeability. On the other hand, diamagnetic materials, owing to their weak magnetic properties, display a negative slope that is less than vacuum permeability when subjected to a magnetic field.

Magnetostriction is derived from the magnetic properties of the material itself. In the experiments conducted, this phenomenon was consistently observed regardless of the applied current, clearly illustrating the relationship between strain and magnetic field strength. The magnetostrictive resonance was further studied to gain a deeper understanding of magnetostriction concepts.

In conclusion, the experiments detailed in this report are crucial for understanding material science and the magnetic properties of materials. The B-H curve measurements provide insights into the unique characteristics of different magnetic materials, even if they appear similar. Additionally, the magnetostriction measurements can detect minute changes in material dimensions using a strain gauge, which uses inexpensive electronic components and relatively simple circuitry, making the experiment more feasible.

Work Cited

Bian, L., Wen, Y., Li, P., Wu, Y., Zhang, X., & Li, M. (2016). Magnetostrictive stress induced frequency shift in resonator for magnetic field sensor. Sensors and Actuators A: Physical, 247, 453–458. https://doi.org/10.1016/j.sna.2016.06.041

Dhanyaprabha, K. C., Jacob, B., Mohan, M., Al-Omari, I. A., Al-Harthi, S. H., Myint, M. T. Z., & Thomas, H. (2023). Investigation on the effect of magnetostriction on the magnetoelectric coupling of BaTiO3 - Ni(1-x) Zn(x) Fe2O4 multiferroic particulate composites. Materials Science and Engineering: B, 298, 116859. https://doi.org/10.1016/j.mseb.2023.116859

Ekreem, N. B., Olabi, A. G., Prescott, T., Rafferty, A., & Hashmi, M. S. J. (2007). An overview of magnetostriction, its use and methods to measure these properties. Journal of Materials Processing Technology, 191(1–3), 96–101. https://doi.org/10.1016/j.jmatprotec.2007.03.064

Pacewicz, A., Krupka, J., Mikkelsen, J. H., Lynnyk, A., & Salski, B. (2023). Accurate measurements of the ferromagnetic resonance linewidth of single crystal BaM hexaferrite spheres employing magnetic plasmon resonance theory. Journal of Magnetism and Magnetic Materials, 580, 170902. https://doi.org/10.1016/j.jmmm.2023.170902

Plouffe, B. D., Murthy, S. K., & Lewis, L. H. (2014). Fundamentals and application of magnetic particles in cell isolation and enrichment: a review. Reports on Progress in Physics, 78(1), 016601. https://doi.org/10.1088/0034-4885/78/1/016601

Storr, W. (2023, January 26). Magnetic Hysteresis Loop including the B-H Curve. Basic Electronics Tutorials. https://www.electronics-tutorials.ws/electromagnetism/magnetic-hysteresis.html

Xu, Y., & Shang, X. (2019). Vibration of magnetostrictive composite cantilever actuator. Materials Research Express, 6(4), 046105. https://doi.org/10.1088/2053-1591/aafc67

Yalcin, O. (2013). *Ferromagnetic resonance: Theory and applications*. IntechOpen.